Band-edge structure of indium-doped $Pb_{1-x}Sn_xTe$ across the band-inversion region investigated by the far-infrared magnetoplasma method

S. Takaoka, S. Shimomura,* H. Takahashi, and K. Murase
Department of Physics, Faculty of Science, Osaka University, 1-1 Machikaneyama-cho, Toyonaka-shi, Osaka 560, Japan
(Received 26 April 1989)

Far-infrared magnetoplasma spectra in 1 at.% indium-doped $Pb_{1-x}Sn_xTe$ single crystals are measured across the band-inversion region ($0.15 < x < 0.40$) at temperatures between 4.2 and 20 K, where a large photoconductivity change is observed. From the photocarrier concentration dependences of effective masses, the band-edge mass and the band gap are determined with use of the two-band model. It is found that the band gaps do not change appreciably by doping indium, while the edge masses become much heavier as compared with those of undoped $Pb_{1-x}Sn_xTe$. It seems that the band-edge masses and the energy gaps do not reach zero at the band-inversion tin composition ($x \simeq 0.35$).

I. INTRODUCTION

Lead-tin telluride ($Pb_{1-x}Sn_xTe$) is one of the well-known narrow-band-gap semiconductors.[1] It has been believed that the band gap (E_g) decreases with increasing x and the conduction and valence bands cross each other, i.e., E_g becomes zero near $x = 0.35$ at 4.2 K and then increases again with larger x.[2] However, it is very difficult to determine the band-edge structure near the band-inversion region, since only high-carrier concentration specimens (more than 10^{18} cm^{-3}) are available due to the deviation from the stoichiometric composition,[3] and the band-edge structure is hidden by the high-carrier concentration and the low density of states due to the small effective mass. It is known that the chemical potential (Fermi level) of In-doped (1 at.%) $Pb_{1-x}Sn_xTe$ ($Pb_{1-x}Sn_xTe$:In) is pinned by In impurities.[4,5] The Fermi level moves down from the conduction band ($x < 0.23$) to the band-gap region ($0.23 < x < 0.30$) and then to the valence band ($x > 0.30$) with increasing x as shown in Fig. 1.[5] The low-carrier-concentration specimens with 10^{15}–10^{17} cm^{-3} are obtained across the band-inversion region. Furthermore, a remarkable strong photoconduction sensitive to infrared radiation is observed below 20 K, as shown in Fig. 2.[5,6] With changing temperature between 4.2 and 20 K, the photocarrier concentration varies greatly. We can obtain the information of band parameters such as effective mass, etc., in a wide range of carrier concentration in the In-doped specimen.

The origin of the Fermi-level pinning and the large photoconductivity due to In impurities is explained by the Anderson negative-U model at present as follows.[5,7,8] The In ions in $Pb_{1-x}Sn_xTe$ can be in three different states as unoccupied, singly occupied, and doubly occupied. Since the trapped carriers at In ions couple strongly with the surrounding lattice with a large lattice relaxation, the energy of the doubly occupied state ($E_0 - U$) becomes lower than that of the singly occupied state (E_0). If there are no other impurities and/or defects, the chemical potential is fixed at $E_0 - U/2$.[9] The chemical potential (E_F) is determined by the thermal equilibrium condition among the singly and doubly occupied states and band electrons (holes) near the band edge. The Fermi level is almost fixed at $E_0 - U/2$ as long as the In-impurity concentration (1 at.%) is much higher than that of the remaining impurities and defects. The present experiment satisfies the condition. The large photoconductivity at low temperatures is also explained based on this model.[5] The photoexcited carriers in the conduction (valence) band cannot easily return to the original impurity states, because there exists an energy barrier between the conduction band and the impurity state caused by the lattice relaxation at the impurity. Once electrons are excited from the impurities, the photocarriers excited in the conduction band are accumulated due to a long relaxation time at low temperatures. With raising temperatures, the photocarriers can get over the barrier more easily due to a larger thermal energy, and the photocarrier concentration decreases. Owing to In impurities, various phenomena such as the Shubnikov–de Haas–type oscillation of carrier concentration,[10,11] a sign inversion of the Hall coefficient with respect to the magnetic field,[5,10] and the avalanchelike I-V characteristics,[12] etc., have been observed.

By taking advantages of low carrier concentration and large change of photocarriers in $Pb_{1-x}Sn_xTe$:In ($0.15 < x < 0.40$), we have investigated the band-edge structure by the far-infrared magnetoplasma method.[13]

II. EXPERIMENTAL PROCEDURE

The specimens used in this experiment were single crystals grown by a vapor-transport method. As-grown crystals were cut into slices with (100) surface and they were isothermally annealed in In vapor with Ar gas with decreasing temperatures stepwise.[5] The doping concentration of In was estimated to be about 1 at. %. The far-infrared light sources were an HCN laser with 337 μm in wavelength and the optically pumped gas laser with 163, 184, 394, 419, and 433 μm in wavelength. The laser light

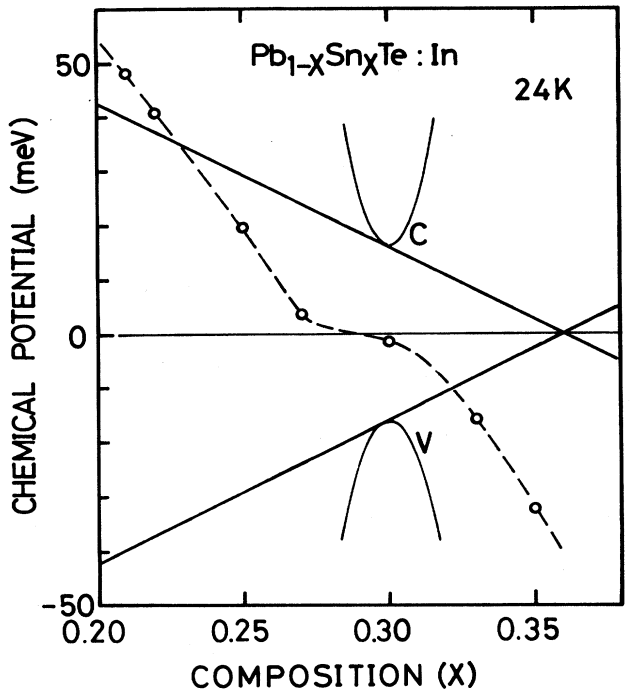

FIG. 1. Tin composition (x) dependences of chemical potential of In-doped $Pb_{1-x}Sn_xTe$ together with conduction- and valence-band edge at 24 K.

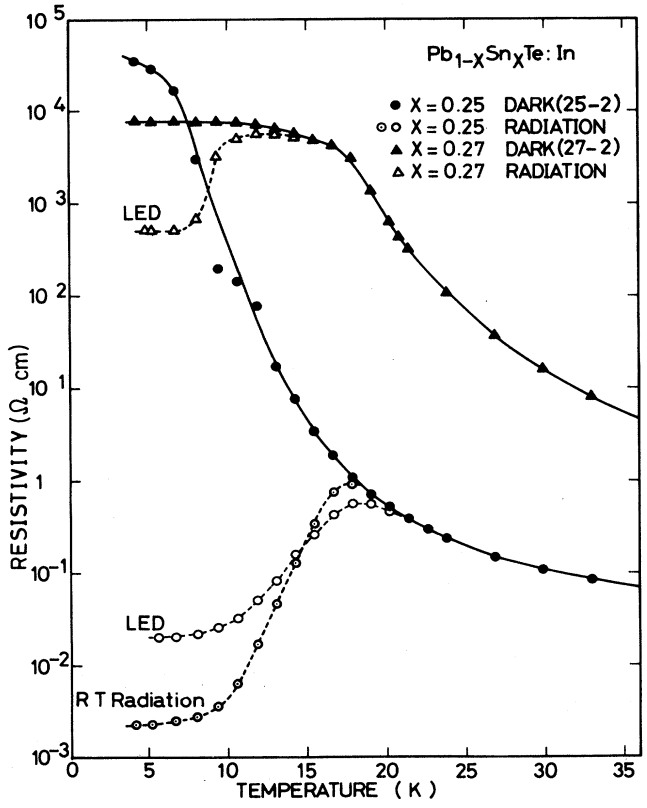

FIG. 2. Temperature dependences of resistivities in In-doped $Pb_{1-x}Sn_xTe$ at low temperatures ($x=0.25$ and 0.27) with and without radiation. LED: illumination from photodiode. RT radiation: room-temperature radiation.

is guided into a stripline and the transmitted light through it was detected by an InSb detector. A horizontal magnetic field up to 4 T was applied to the specimen by the split-type superconducting magnet. The magnetic field direction with respect to the specimen could be changed from $\langle 001 \rangle$ to $\langle 110 \rangle$ by rotating the stripline.[14,15] The specimens were exposed to a room-temperature blackbody radiation.

III. MAGNETOPLASMA THEORY IN $Pb_{1-x}Sn_xTe$

The conduction-band minima and the valence-band maxima of $Pb_{1-x}Sn_xTe$ are located at the L points in the Brillouin zone. There are four elongated Fermi surfaces at the $\langle 111 \rangle$ valley and the other three equivalent valleys. According to the magnetoplasma theory in the Drude model, the effective dielectric functions (ϵ^*) in the Faraday configuration ($\mathbf{B} \| \mathbf{q} \| \langle 001 \rangle$) and the Voigt configuration ($\mathbf{B} \| \langle 110 \rangle$, $\mathbf{q} \| \langle 001 \rangle$) are expressed, respectively, as Eqs. (1) and (2) as follows:[15]

$$\epsilon^*_{CRA}=\epsilon_{xx}-i\epsilon_{xy} \quad \text{and} \quad \epsilon^*_{CRI}=\epsilon_{xx}+i\epsilon_{xy} , \tag{1}$$

where ϵ_{xx} and ϵ_{xy} are given in the Appendix. Consider the following:

$$\epsilon^*_E=\epsilon_{yy}+\epsilon^2_{yz}/\epsilon_{zz} \quad \text{and} \quad \epsilon^*_O=\epsilon_{xx} , \tag{2}$$

where ϵ_{xx}, ϵ_{yy}, ϵ_{zz}, and ϵ_{yz} are given in the Appendix. The reflectivity (R) is calculated from the effective dielectric function as

$$R=\frac{1}{2}\left[\left|\frac{(\epsilon^*_+)^{1/2}-1}{(\epsilon^*_+)^{1/2}+1}\right|^2+\left|\frac{(\epsilon^*_-)^{1/2}-1}{(\epsilon^*_-)^{1/2}+1}\right|^2\right] , \tag{3}$$

where $\epsilon^*_+=\epsilon^*_{CRI}$ and $\epsilon^*_-=\epsilon^*_{CRA}$ for the Faraday configuration, and $\epsilon^*_+=\epsilon^*_O$ and $\epsilon^*_-=\epsilon^*_E$ for the Voigt configuration.

Since the reflectivity from the specimen in the far-infrared region is near 100% and its change by magnetic field is very small, we used the strip-line method, which gives a strong contrast over change of reflection due to multiple reflection of the incident light through the narrow space between the specimen and metal. Strictly speaking, the transmission spectra from the strip line have to be analyzed taking into account the mode problem in the same way as in the wave guide. This problem has been solved and the calculated transmission spectra is almost the same as that based on multiple reflection.[15] Therefore we used the nth power of reflectivity (R^n) calculated from the effective dielectric functions [Eqs. (1) and (2)] in the analyses of the transmission spectra.

IV. EXPERIMENTAL RESULTS AND ANALYSIS

In Figs. 3 and 4, the magnetic field dependences of transmission spectra in the Faraday and the Voigt configurations, respectively, for $Pb_{1-x}Sn_xTe$:In ($x=0.23$) are shown with various laser wavelengths at 4.2 K. The dashed curves are the calculated spectra from the multiple-reflection model as described before. The dips in the spectra correspond to the dielectric anomalies ($\epsilon^*=1$), since the laser wavelengths used in these mea-

surements are in the reststrahlen region (18–114 cm^{-1}) and the lattice dielectric function (ϵ_L) of $Pb_{1-x}Sn_xTe$ is negative. The carrier concentration, the transverse and longitudinal masses, and the TO-phonon frequency have been determined from the laser-wavelength dependence of the spectra. The temperature dependence of magneto-plasma transmission spectra with $\lambda=337$ μm laser light are shown in Figs. 5 and 6. With increasing temperatures from 4.2 to 20 K, the dips become smaller and their positions shift to lower magnetic fields due to the reduction of photocarrier concentration and cyclotron mass. The temperature dependence of the photocarrier concentration is discussed qualitatively based on the Anderson negative-U mode in other papers.[16,17] By fitting these spectra to the calculated ones, the photocarrier concentration and the band mass have been determined for each temperature. We have replotted these obtained band parameters as the photocarrier concentration dependence of the transverse mass (m_t^*) in Fig. 7.

The effective mass becomes smaller with decreasing carrier concentrations as shown in Fig. 7 due to the band nonparabolicity. Since the band gaps (E_g) of the present specimens ($0.15<x<0.40$) are very small ($E_g<80$ meV), the two-band-model theory is applicable to describe the band-edge structure. According to the two-band theory, the effective mass (m^*) with energy E is expressed as[18]

$$m^*=m_0(1+2E/E_g)\ , \tag{4}$$

where m_0 is the band-edge mass. The carrier concentration (N) by the two-band theory is given as

$$N=\int D(E)f(E,T)dE\ , \tag{5}$$

where $D(E)$ and $f(E,T)$ are the density of states and the Fermi distribution function, respectively, and are expressed as

$$D(E)=\frac{1}{2\pi^2}(m_{t0}^2m_{l0})^{1/2}(2/\hbar^2)^{3/2} \times[E(1+E/E_g)]^{1/2}(1+2E/E_g) \tag{6}$$

and

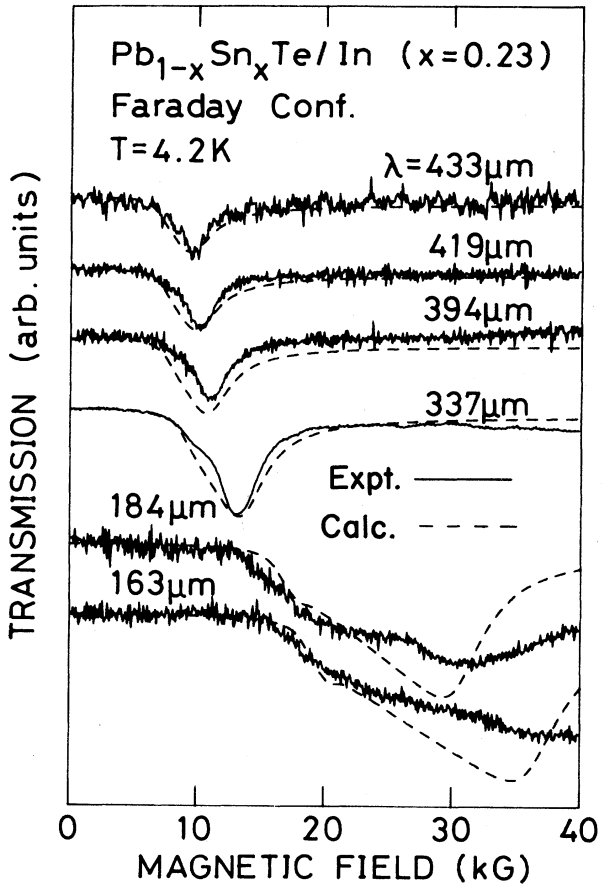

FIG. 3. Magnetic field dependences of strip-line transmission spectra in In-doped $Pb_{1-x}Sn_xTe$ ($x=0.23$) in Faraday configuration at 4.2 K with various laser wavelengths. Solid and dotted curves are measured and calculated spectra, respectively.

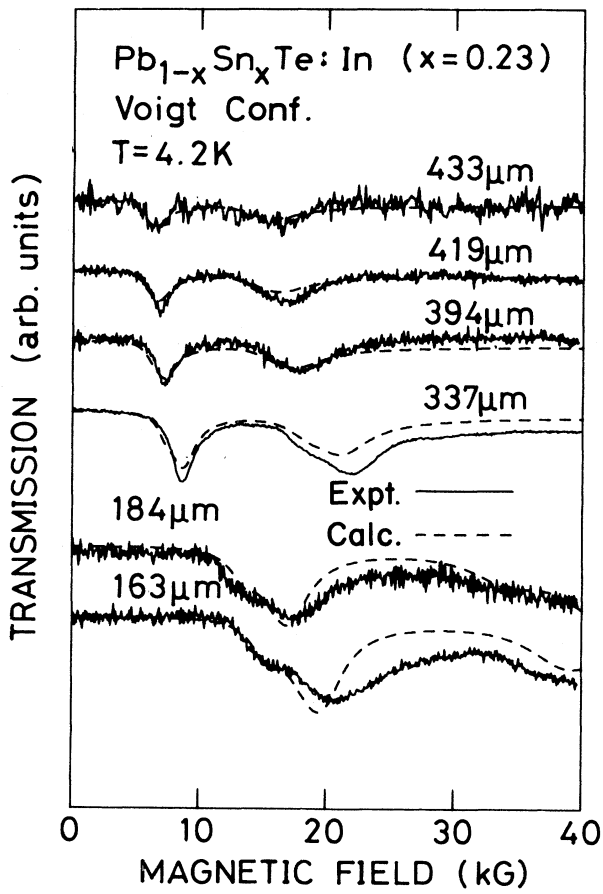

FIG. 4. Magnetic field dependences of strip-line transmission spectra in In-doped $Pb_{1-x}Sn_xTe$ ($x=0.23$) in Voigt configuration at 4.2 K with various laser wavelengths. Solid and dotted curves are measured and calculated spectra, respectively.

$$f(E,T)=\frac{1}{1+\exp[(E-E_F)/k_BT]}\ , \tag{7}$$

where m_{t0} and m_{l0} are the transverse and longitudinal effective mass at the band edge, respectively. The energy (E) in Eq. (4) which most effectively contributes to the cyclotron-resonance transition is considered to be the maximum of the function

$$D(E)f(E,T)D(E+\hbar\omega_c)[1-f(E+\hbar\omega_c,T)]\ , \tag{8}$$

where $\hbar\omega$ is the incident laser energy (3.7 meV for $\lambda=337$ μm).

We have calculated the carrier-concentration dependence of the effective mass from Eqs. (4)–(8) as shown by the solid line in Fig. 7. The adjustable parameters are E_g and m_{t0} in this fitting. The other parameters such as TO-phonon frequency, etc., have little influence on the calculations. Strictly speaking, E_g and m_{t0} vary slightly between 4.2 and 20 K. The amount of variation is estimated to be small enough to neglect due to the saturation effect of temperature dependence of E_g and m_{t0} at low temperatures ($E_g<3$ meV).[19] We have determined E_g and m_{t0} of $Pb_{1-x}Sn_xTe$:In for various x as shown in Figs. 8 and 9, respectively. The dashed lines in these figures are the extrapolated values of undoped $Pb_{1-x}Sn_xTe$ from the experiments with smaller x.[5,20] The solid circles in Fig. 9 are the effective masses with $N=5.5\times10^{17}$ cm^{-3} for $x=0.15$ and $N=3.7\times10^{17}$ cm^{-3} for $x=0.40$, respectively, because the variations of carrier concentrations with temperatures in these specimens are not enough to determine the band-edge masses. The band-edge masses in these specimens are smaller than the solid circles.

V. DISCUSSION

As seen from these figures, m_0 are much heavier than those of undoped $Pb_{1-x}Sn_xTe$, while E_g do not change remarkably except in the band-inversion region. According to the two-band theory, the band-edge mass (m_0) is expressed as[18]

$$m_0=E_g/2P^2\ , \tag{9}$$

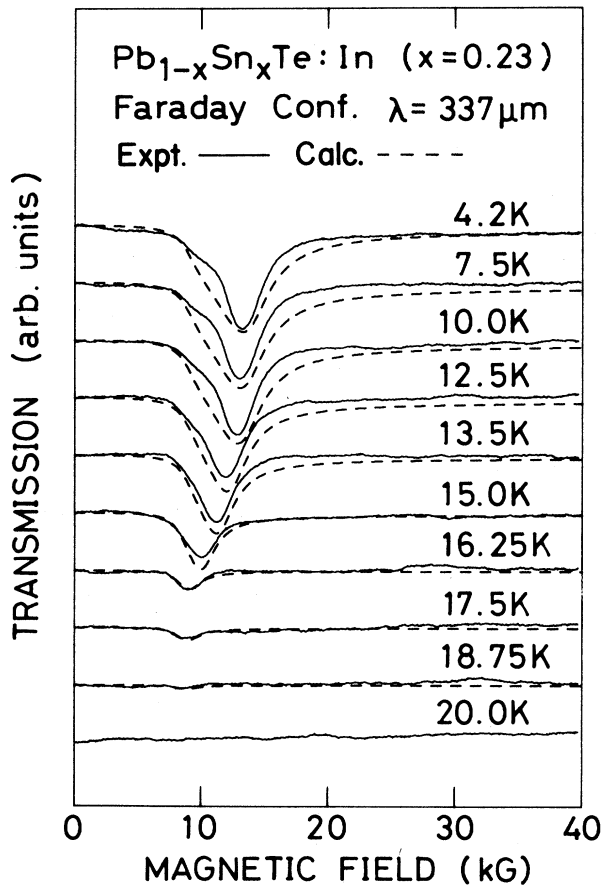

FIG. 5. Magnetic field dependences of strip-line transmission spectra ($\lambda=337$ μm) in In-doped $Pb_{1-x}Sn_xTe$ ($x=0.23$) in Faraday configuration at temperatures between 4.2 and 20 K. Solid and dotted curves are measured and calculated spectra, respectively.

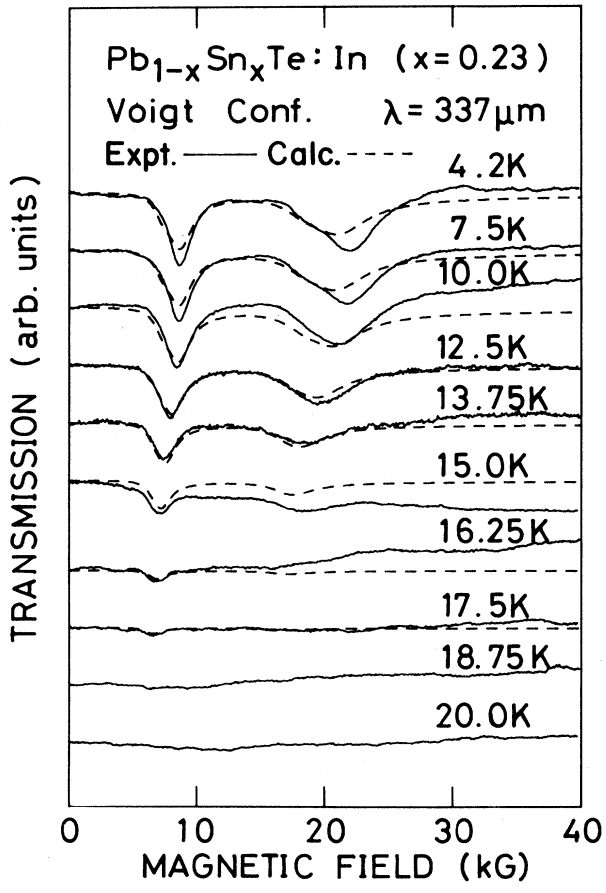

FIG. 6. Magnetic field dependences of strip-line transmission spectra ($\lambda=337$ μm) in In-doped $Pb_{1-x}Sn_xTe$ ($x=0.23$) in Voigt configuration at temperatures between 4.2 and 20 K. Solid and dotted curves are measured and calculated spectra, respectively.

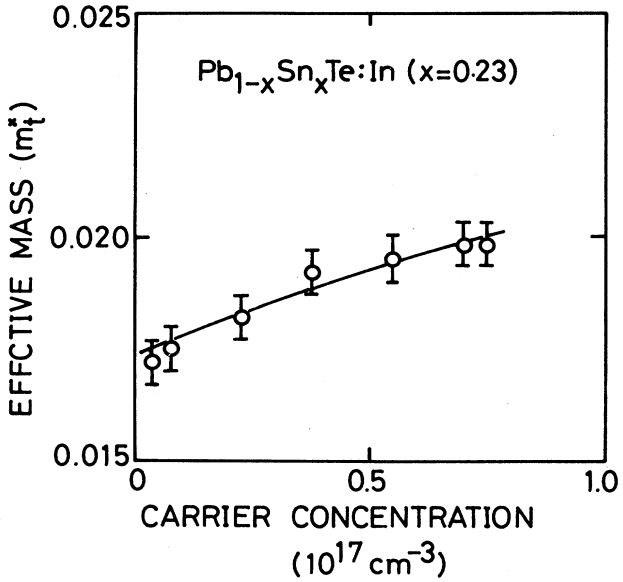

FIG. 7. Photocarrier concentration dependence of transverse effective mass in In-doped $Pb_{1-x}Sn_xTe$ ($x=0.23$). Solid curve is calculated from two-band model. The fitting parameters are energy gap (E_g) and transverse band-edge mass (m_{to}).

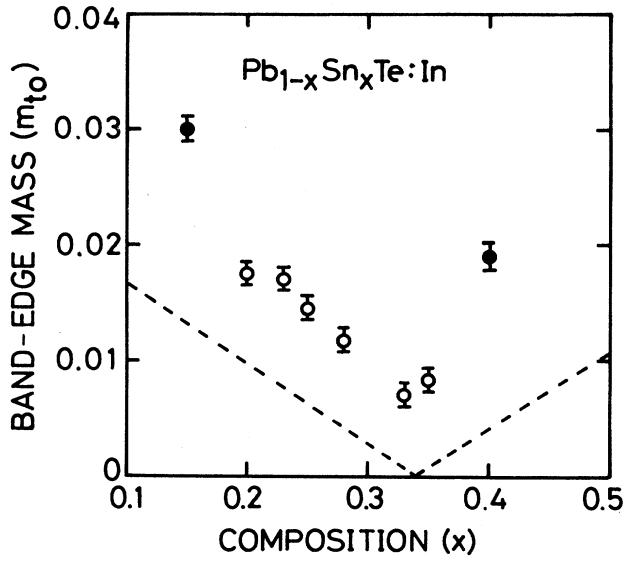

FIG. 9. Tin composition (x) dependence of transverse band-edge mass (open circles) in In-doped $Pb_{1-x}Sn_xTe$. Solid circles are, respectively, transverse effective masses with $N=5.5\times10^{17}$ cm^{-3} for $x=0.15$ and $N=3.7\times10^{17}$ cm^{-3} for $x=0.40$. Dashed line is expected band-edge mass of undoped $Pb_{1-x}Sn_xTe$.

where P is the momentum matrix element between the conduction and valence bands. The enhancement of m_0 by doping In was already observed in a $Pb_{1-x}Sn_xTe$ film specimen.[21] However, there are some complicated situations, such as the valley splitting due to the strain in the film caused by the mismatch between the film and the substrate, and only one specimen was measured. We could not trace the enhancement effect to its origin. From the present investigation, it may be concluded that the enhancement of m_0 by doping In impurities is mainly due to the reduction of the matrix element.

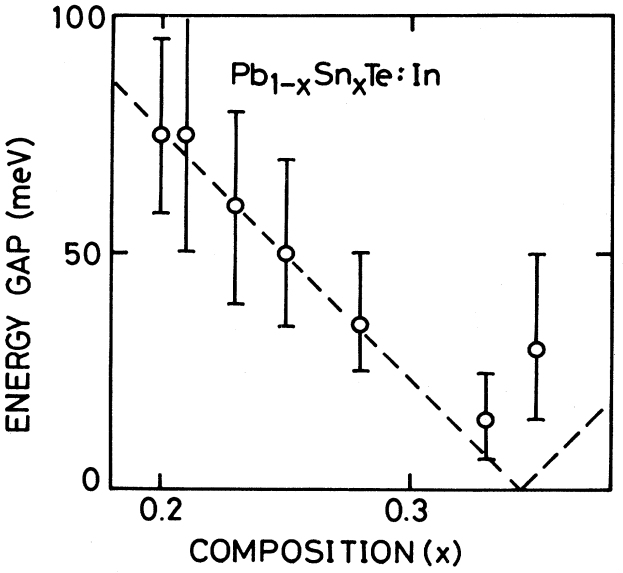

FIG. 8. Tin composition (x) dependence of E_g in In-doped $Pb_{1-x}Sn_xTe$. Dashed line is expected value of undoped $Pb_{1-x}Sn_xTe$.

The reason why the matrix element is reduced by In impurities is unclear at present. However, there are a few discussions about it, as follows. One of the possibilities of enhancing m_0 is the polaron effect.[22,23] A strong evidence of the polaron effect would be observation of a measured frequency dependence of the effective mass. But an appreciable frequency dependence has not been observed between 23 and 61.3 cm^{-1}, as shown in Figs. 3 and 4. The local vibration mode of In atoms in $Pb_{1-x}Sn_xTe$ was observed at 160 cm^{-1} by the far-infrared-absorption measurement.[24] The measured frequency range is far from the local-mode frequency and the frequency dependence may be too small to observe. Another possibility is that the matrix element is reduced by the static potential of In ions.

It is also very interesting to know whether E_g and m_0 become really zero or not in the band-inversion region. As seen in Figs. 8 and 9, it seems that m_0 do not reach zero, and the conduction and valence bands do not cross, but instead repel each other at finite E_g. In the perfect crystal, it is expected that E_g can be zero from group theory.[2,25] Substituting Sn for Pb and/or the doping In impurities will break the crystal symmetry and the two bands might repel each other. It is very difficult to say whether the nonzero effect of E_g and m_0 is essential in $Pb_{1-x}Sn_xTe$ or as a result of doping In from this measurement. We cannot reach a definite conclusion about this problem at present. It would be important to investi-

gate the doping In concentration dependence of the band-edge parameters. Further systematic investigations are necessary to make clear the band-edge structure at the band-inversion point and the anomalous effect of In impurities.

VI. SUMMARY AND CONCLUSION

The band-edge structures (m_0 and E_g) of $Pb_{1-x}Sn_xTe$:In across the band-inversion region were determined by the far-infrared magnetoplasma reflection method using a large amount of change of photocarrier concentration. By doping In ($\simeq 1$ at. %), E_g are not different from the expected values of undoped $Pb_{1-x}Sn_xTe$, while m_0 become much heavier than those of undoped $Pb_{1-x}Sn_xTe$. From these results and the two-band model, it was concluded that the momentum matrix element between the conduction and valence bands is reduced by doping In. Some origins about the reduction and the band-edge structures at the band-inversion region were discussed.

ACKNOWLEDGMENTS

The authors would like to thank T. Itoga for the sample preparations. One of the authors (S.T.) was supported by the 10th Nippon Sheet Glass Foundation for Materials Science, and another (K.M.) by the 22nd Science and Technology of Toray Science Foundation.

APPENDIX

In the Faraday configuration ($\mathbf{B}\|\mathbf{z}\|\langle 001\rangle$ and $\mathbf{q}\|\mathbf{z}$), the dielectric tensors of $Pb_{1-x}Sn_xTe$ are given by the Drude model as

$$\epsilon_{xx}=\epsilon_L-\frac{4\pi Ne^2}{m_t}\frac{1}{3}\frac{2K+1}{K}\frac{1}{\omega}\frac{\omega+i\Gamma}{(\omega+i\Gamma)^2-\omega_c^2},$$

and

$$\epsilon_{xy}=i\frac{4\pi Ne^2}{m_t}\left[\frac{K+2}{3K}\right]^{1/2}\frac{I}{\omega}\frac{\omega+i\Gamma}{(\omega+i\Gamma)^2-\omega_c^2},$$

where $K=m_l/m_t$ is the anisotropy ratio of the transverse and longitudinal effective mass, $\omega_c=eB/m_tc[(K+2)/3K]^{1/2}$, and Γ is the reciprocal of the relaxation time of carriers.

In the Voigt configuration ($\mathbf{B}\|\mathbf{x}\|\langle 110\rangle$ and $\mathbf{q}\|\mathbf{z}$), the dielectric tensors of $Pb_{1-x}Sn_xTe$ are given by the Drude model as

$$\epsilon_{xx}=\epsilon_L-\frac{2\pi Ne^2}{m_t}\frac{1}{\omega(\omega+i\Gamma)}\frac{2K+4}{2K+1}$$
$$-\frac{2\pi Ne^2}{m_t}\left[\frac{K+2}{3K}-\frac{3}{2K+1}\right]\frac{1}{\omega}\frac{\omega+i\Gamma}{(\omega+i\Gamma)^2-\omega_{ca}^2},$$

$$\epsilon_{yy}=\epsilon_L-\frac{2\pi Ne^2}{m_t}\frac{1}{\omega}\frac{\omega+i\Gamma}{(\omega+i\Gamma)^2-\omega_{ca}^2}$$
$$-\frac{2\pi Ne^2}{m_t}\frac{1}{\omega}\frac{K+2}{3K}\frac{\omega+i\Gamma}{(\omega+i\Gamma)^2-\omega_{cb}^2},$$

$$\epsilon_{zz}=\epsilon_L-\frac{4\pi Ne^2}{m_t}\frac{1}{\omega}\frac{2K+1}{3K}\frac{\omega+i\Gamma}{(\omega+i\Gamma)^2-\omega_{ca}^2},$$

and

$$\epsilon_{yz}=-\frac{2\pi Ne^2}{m_t}\frac{1}{\omega}\left[\left[\frac{2K+1}{3K}\right]^{1/2}\frac{\omega_{ca}^2}{(\omega+i\Gamma)^2-\omega_{ca}^2}-\left[\frac{1}{K}\right]^{1/2}\frac{\omega_{cb}^2}{(\omega+i\Gamma)^2-\omega_{cb}^2}\right],$$

where

$$\omega_{ca}=\frac{eB}{m_tc}\left[\frac{2K+1}{3K}\right]^{1/2}\quad\text{and}\quad\omega_{cb}=\frac{eB}{m_tc}\left[\frac{1}{K}\right]^{1/2}.$$

---

*Present address: Department of Material Physics, Faculty of Engineering Science, Osaka University, 1-1 Machikaneyama-cho, Toyonaka-shi, Osaka 560, Japan.

[1]G. Nimtz and B. Schricht, in *Narrow-Gap Semiconductors* (Springer-Verlag, Berlin, 1983), p. 1.

[2]J. O. Dimmock, in *The Physics of Semimetals and Narrow Gap Semiconductors,* edited by D. L. Carter and R. T. Bate (Pergamon, Oxford, 1971), p. 319.

[3]T. C. Harman, J. Nonmetals **1**, 183 (1973).

[4]B. A. Akimov, L. I. Ryabova, O. B. Yatsenko, and S. M. Chudinov, Fiz. Tekh. Poluprovodn. **13**, 752 (1979) [Sov. Phys.—Semicond. **13**, 441 (1979)].

[5]S. Takaoka, T. Itoga, and K. Murase, Jpn. J. Appl. Phys. **23**, 216 (1984).

[6]B. M. Vul, I. D. Voronova, G. A. Kalyuzhnaya, T. S. Mamedov, and T. Sh. Ragimova, Pis'ma Zh. Eksp. Teor. Fiz. **29**, 21 (1979) [JETP Lett. **29**, 18 (1979)].

[7]Yu. V. Andreev, K. I. Geiman, I. A. Drabkin, A. V. Matveenko, E. A. Mozhaev, and B. Ya. Moizhes, Fiz. Tekh. Poluprovodn. **9**, 1873 (1975) [Sov. Phys.—Semicond. **9**, 1235 (1975)].

[8]C. M. Penchina, A. Klein, and K. Weiser, in Proceedings of 15th International Conference on Physics of Semiconductors, Kyoto, 1980 [J. Phys. Soc. Jpn. Suppl. A **49**, 789 (1980)].

[9]D. Adler and E. J. Yoffa, Phys. Rev. Lett. **36**, 1197 (1976).

[10]K. Murase, S. Takaoka, T. Itoga, and S. Ishida, in *Application of High Magnetic Fields in Semiconductor Physics,* Vol. 177 of *Lecture Notes in Physics,* edited by G. Landwehr (Springer-Verlag, Berlin, 1982), p. 374.

[11]S. Takaoka, T. Itoga, and K. Murase, Solid State Commun. **46**, 287 (1983).

[12]B. A. Akimov, N. B. Brandt, B. S. Kerner, V. N. Nikiforov, and S. M. Chudinov, Solid State Commun. **43**, 31 (1982).

[13]S. Takaoka, S. Shimomura, H. Takahashi, and K. Murase, in *Digest of 13th International Conference on Infrared and Mil-*

limeter Waves, Honolulu, 1988, edited by R. J. Temkin (SPIE, Bellingham, 1988), p. 401.

[14]U. Strom, H. D. Drew, and J. F. Koch, Phys. Rev. Lett. **26**, 1110 (1971).

[15]T. Ichiguchi, Dr. thesis, Osaka University, 1981; T. Ichiguchi, S. Nishikawa, and K. Murase, Solid State Commun. **34**, 309 (1980).

[16]S. Shimomura, H. Takahashi, S. Takaoka, and K. Murase, in *Proceedings of the 19th International Conference on the Physics of Semiconductors, Warsaw, 1988,* edited by W. Zawadski (Institute of Physics, Polish Academy of Sciences, Warsaw, 1988), p. 1131.

[17]S. Shimomura, H. Takahashi, S. Takaoka, and K. Murase, in Proceedings of the 15th International Conferences on Defects in Semiconductors, Budapest, 1988, edited by G. Ferenczi [Mater. Sci. Forum **38-14**, 531 (1989)].

[18]P. A. Wolf, J. Phys. Chem. Solids **25**, 1057 (1964).

[19]S. Takaoka and K. Murase, J. Phys. Soc. Jpn. **51**, 1857 (1982).

[20]C. R. Hew, M. S. Adler, and S. D. Senturia, Phys. Rev. B **7**, 5195 (1973).

[21]S. Takaoka, T. Hamaguchi, S. Shimomura, and K. Murase, in *Proceedings of the 17th International Conference on the Physics of Semiconductors, San Francisco, 1984,* edited by J. D. Chadi and W. A. Harrison (Springer-Verlag, New York, 1985), p. 663.

[22]G. Ascarelli, in *Polaron and Exciton,* edited by C. K. Kuper and G. D. Whitfield (Plenum, New York, 1963), p. 365.

[23]H. Burkhard, G. Bauer, P. Grosse, and A. Lopez-Otero, Physica B+C **89B**, 22 (1977).

[24]S. Takaoka and K. Murase, J. Phys. Soc. Jpn. **52**, 25 (1983).

[25]D. L. Mitchell and R. F. Wallis, Phys. Rev. **151**, 581 (1966).